



Global phase diagrams of frustrated quantum antiferromagnets in two dimensions: Doubled Chern-Simons theory

Cenke Xu and Subir Sachdev

Department of Physics, Harvard University, Cambridge, Massachusetts 02138, USA

(Received 22 November 2008; published 6 February 2009)

We present a general approach to understanding the quantum phases and phase transitions of quantum antiferromagnets in two spatial dimensions. We begin with the simplest spin-liquid state, the Z_2 spin liquid, whose elementary excitations are spinons and visons, carrying Z_2 electric and magnetic charges, respectively. Their dynamics is expressed in terms of a doubled $U(1)$ Chern-Simons theory, which correctly captures the “topological” order of the Z_2 spin-liquid state. We show that the same theory also yields a description of the variety of ordered phases obtained when one or more of the elementary excitations condense. Field theories for the transitions and multicritical points between these phases are obtained. We survey experimental results on antiferromagnets on the anisotropic triangular lattice, and make connections between their phase diagrams and our results.

DOI: [10.1103/PhysRevB.79.064405](https://doi.org/10.1103/PhysRevB.79.064405)

PACS number(s): 75.10.Jm, 75.50.Ee, 75.45.+j

I. INTRODUCTION

The study of exotic phases of quantum antiferromagnets has received a great impetus by the experimental discovery of a number of candidate $S=1/2$ Mott insulators. The primary aim of our paper is to present an attempt to place the experimentally discovered phases in a single global phase diagram. Such a phase diagram exposes relations between the excitations of the various phases, and leads to theories for the possible quantum phase transitions between them.

As will become clear from our analysis, we can generate distinct “global” phase diagrams for distinct lattice types and exchange interactions in two spatial dimensions. We will present a general method for analyzing these, but will focus on a single lattice type, found in a number of experimental systems: this is the distorted triangular lattice shown in Fig. 1. Thus we are interested in the $S=1/2$ antiferromagnet, with $SU(2)$ -invariant Heisenberg exchange interactions J and J' illustrated in Fig. 1, along with possibly additional longer-range two-spin or multispin exchange interactions which have the same symmetry as Fig. 1. A number of limiting cases of this lattice have been examined earlier, and we will connect with all of these results:

(i) for $J' \ll J$ the model becomes essentially equivalent to the square lattice antiferromagnets considered in Refs. 1–3, and our results agree with these earlier results in this regime;

(ii) for $J \ll J'$ we have the quasi-one-dimensional antiferromagnets which have been studied in some detail by Starykh and co-workers;^{4,5}

(iii) for $J \approx J'$ we have the triangular lattice antiferromagnets for which our results will connect with those of Refs. 6–9;

(iv) Weihong *et al.*¹⁰ performed a series-expansion study for the entire range of J'/J , and obtained phases which will also appear in our phase diagrams;

(v) there have been a number of numerical studies^{11–14} of isotropic triangular lattice case, $J'=J$, but with an additional four-spin ring exchange interaction, and our theory will provide candidate phase diagrams for this model; and

(vi) the nonmagnetic phases for $J'=J$ have been modeled by the quantum dimer model¹⁵ on the triangular lattice by

Moessner and Sondhi,¹⁶ and our theory will also find their phases.

Experimental examples extend over the full range of parameters for the lattice in Fig. 1, and realize a variety of phases:

(a) A remarkable series of experiments was carried out by Kato and co-workers^{17–23} on the organic Mott insulators $X[\text{Pd}(\text{dmit})_2]_2$ (for a general review of the organic compounds, see Ref. 24). Each site of the lattice in Fig. 1 has a pair of $\text{Pd}(\text{dmit})_2$ molecules carrying charge $-e$ and spin $S=1/2$. X ranges over a variety of monovalent cations, and the choice of different X 's allows experiments over a range of values of J'/J . The resulting phase diagram²² has magnetic order with decreasing critical temperatures from $T_c \approx 42$ K to $T_c \approx 15$ K across the compounds $X=\text{Me}_4\text{P}$, Me_4As , EtMe_3As , $\text{Et}_2\text{Me}_2\text{P}$, $\text{Et}_2\text{Me}_2\text{As}$, and Me_4Sb , as the value of J'/J increases from $J'/J \approx 0.35$ to $J'/J \approx 0.7$. (There are uncertainties in the overall scale of J'/J , and there are also likely to be significant four-spin ring exchange terms.) The magnetic order is likely of the two-sublattice Néel type,²² although there are no neutron-scattering observations confirming this. The compound with $X=\text{EtMe}_3\text{Sb}$ has $J'/J \approx 0.85$, has no observable Néel order,²³ and has been suggested to be near the quantum critical point²² at which the Néel order vanishes. Finally, the compound^{20,21} with $X=\text{EtMe}_3\text{P}$ has $J'/J \approx 1.05$ and has a ground state with a spin

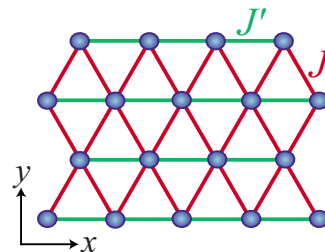


FIG. 1. (Color online) Distorted triangular lattice with nearest-neighbor Heisenberg exchanges J' (on all horizontal bonds) and J (on all other bonds), representing the geometry of systems examined in this paper.

gap and spontaneous columnar valence-bond-solid (VBS) order at low T . The VBS order vanishes at a phase transition observed to be at 25 K, and the low- T spin gap is measured to be ≈ 40 K (the exchange constant $J \approx 250$ K). Thus these series of compounds appear to realize the Néel-VBS transition predicted in Ref. 1, and in this paper we will place this transition in the context of global phase diagrams of models on the lattice in Fig. 1. We also note that a Néel-VBS transition as a function of increasing J'/J has also been found in the series-expansion study.¹⁰

(b) A separate set of experiments has been performed on the organic Mott insulators κ -(ET)₂Z, which also realize the $S=1/2$ antiferromagnet on the lattice in Fig. 1. The compound with $Z=\text{Cu}[\text{N}(\text{CN})_2]\text{Cl}$ has $J'/J \approx 0.5$, and has a ground state with Néel order,²⁵ as found in the Pd(dmit)₂ series above for small J'/J . The organic insulator with $Z=\text{Cu}_2(\text{CN})_3$ has $J'/J \approx 1$, and appears to have no antiferromagnetic or VBS ordering down to the lowest observed temperatures.^{26–29} This is therefore a candidate for a spin-liquid ground state, whose nature has been the subject of recent work.^{13,30–32} The bosonic Z_2 spin-liquid state proposed for this compound in Ref. 32 will appear in our phase diagrams below, and indeed will be natural point of departure for our entire analysis. We believe that the experimental observation, noted above, of the other phases in our phase diagram can be regarded as a point of support for our perspective. We will briefly mention below how Z_2 spin-liquid states with fermionic spinons,³⁰ and other related states, can appear in our approach.

(c) The transition-metal insulator^{33,34} Cs_2CuCl_4 has $S=1/2$ Cu ions on the vertices of the triangular lattice in Fig. 1 with $J \approx J'/3$. The ground state has spiral antiferromagnetic order, similar to that present in the perfect triangular lattice ($J=J'$), and will appear in the phase diagrams below. An approach starting from the quasi-one-dimensional limit $J \ll J'$ has been successfully used^{4,5} to describe the spiral ground state, and also the inelastic-neutron-scattering spectrum at high energies.

As noted above, our point of departure is a Z_2 spin-liquid state. The earliest proposals of such liquids involved BCS-type states of paired charge 0, $S=1/2$ particles (“spinons”) which were either bosons⁶ or fermions.³⁵ Fluctuations about this state are expressed in terms of a Z_2 gauge theory, in which the spinons carry a Z_2 electric charge, and hence the name of the spin liquid. A large number of other models of Z_2 spin liquids have appeared since then.^{16,36–41} We will find it convenient to begin with Z_2 spin liquid in which the elementary spinons are bosons because it is connected naturally to a variety of ordered states found experimentally (which we have described above). We will denote the bosonic spinons by a complex field z_α , where $\alpha = \uparrow, \downarrow$ is a spin index.

Apart from the spinon, the other fundamental elementary excitation of a Z_2 spin liquid is a charge 0 particle carrying Z_2 magnetic flux. This particle was pointed out in Ref. 6, but its particular importance to the physical properties of Z_2 spin liquids was emphasized by Senthil and Fisher,³⁶ who called it a “vison.” In all cases we shall consider that it is possible to combine the real visons into complex scalar fields v_a , where $a=1, \dots, N_v$ is an additional flavor index which depends

upon the nature of the underlying lattice. The visons are bosons, but the spinons and visons have mutual semionic statistics.^{36,42} Consequently, by forming bound states of the bosonic spinons z_α and the visons v_a , we obtain $S=1/2$ spinons which are fermions.⁴² This bound state formation offers a route to extending our analysis to the case of fermionic spinons, but we shall not comment further on this in the present paper.

Our starting point is an effective-field theory for the spinons z_α and the visons v_a which implements their mutual semionic statistics. As discussed generally by Freedman *et al.*³⁹ and implemented more specifically in Z_2 spin liquids with fermionic spinons by Kou *et al.*,⁴³ this mutual statistics can be realized by a doubled U(1) Chern-Simons (CS) theory. A similar formalism was also applied to the cuprates, with mutual statistics between spin and charge degrees of freedom.⁴⁴ To this end, we introduce two U(1) gauge fields, a_μ and b_μ , and will consider effective Lagrangians with the following schematic structure in 2+1 space-time dimensions:

$$\mathcal{L} = \sum_{\alpha=1}^2 \{ |(\partial_\mu - ia_\mu)z_\alpha|^2 + s_z |z_\alpha|^2 \} + \sum_{a=1}^{N_v} \{ |(\partial_\mu - ib_\mu)v_a|^2 + s_v |v_a|^2 \} + \frac{ik}{2\pi} \epsilon_{\mu\nu\lambda} a_\mu \partial_\nu b_\lambda + \dots, \quad (1.1)$$

where $\mu, \nu, \lambda = x, y, \tau$ are space-time indices, and s_z and s_v are the primary couplings we will tune to obtain our global phase diagrams. The integer $k=2$ implements the needed semionic statistics. The ellipses represent additional terms in the effective potential for the z_α and v_a which are constrained by the projective symmetry group (PSG), i.e., the transformations of the spinons and visons under the symmetries of the lattice spin Hamiltonian. We will discuss these terms more carefully when we describe the different PSGs in the body of the paper.

In passing, we note that supersymmetric versions of the doubled Chern-Simons theory in Eq. (1.1) have recently been the focus of intense interest in the string theory literature.^{45–50} Their model of interest is⁴⁷ a Chern-Simons theory with a $U(N) \times U(N)$ gauge group, with opposite signs for the Chern-Simons term for the two $U(N)$'s, and with matter fields which are bifundamentals in the $U(N)$'s. Equation (1.1) is also precisely of this form with $N=1$: we can define $c_\mu = a_\mu + b_\mu$ and $d_\mu = a_\mu - b_\mu$, and then the c_μ and d_μ fields have diagonal Chern-Simons terms with opposite signs, and the z_α and v_a carry bifundamental charges. The $U(N) \times U(N)$ theories have been argued^{48,49} to be dual to M theory on $AdS_4 \times S^7/Z_k$, which is reason for the interest. The $N=1$ case with $N=4$ supersymmetry has been argued⁵⁰ to be exactly dual to a U(1) gauge theory without a Chern-Simons terms (the latter theory was reviewed in Ref. 51). The analogs of such $N=1$ dualities for nonsupersymmetric theories are well known in the condensed-matter literature, and we will discuss examples in the present paper (see also Ref. 36).

A natural question arises at this point: what are the conditions under which it is permissible to implement a U(1) CS

theory realization of the Z_2 spin liquid, rather than directly in terms of a Z_2 gauge theory? When we are discussing the topological properties of the ground state or single-quasiparticle excitations, there does not appear to be any obstacle to using a $U(1)$ theory.⁴³ However, the issue becomes more delicate when the excitations proliferate, and we are considering quantum phase transitions out of the spin-liquid state. This question is discussed further in Sec. VI, where we will find examples of transitions at which our $U(1)$ CS description fails. However, we also find cases where it does succeed, and these are the main focus of this paper. As we will see in Sec. IV, for these successful cases, because of the constraints of the lattice PSG, the lowest-order terms which break either of the $U(1)$ gauge invariances of Eq. (1.1) are of eighth order, $\sim v_a^8$ as in Eq. (4.2). Their effects are easily incorporated into our analysis as a soft symmetry breaking. We mention that the connection between doubled Z_2 and $U(1)$ CS theories was also discussed by Balents and Fisher⁵² in a different context.

Crucial to our analysis will be exact results on the low-energy spectrum of \mathcal{L} on a $L \times L$ torus as a function of s_z and s_v . For the case where both s_v and s_z are large and positive, both the spinons and visons are gapped, and we realize a Z_2 spin liquid. Here we can integrate out the z_α and v_a , and are left with a pure doubled CS gauge theory. This theory was quantized exactly on a torus in Refs. 39 and 43. The key variables in this quantization were the fluxes piercing the two cycles $C_{x,y}$ of the torus

$$A_i = \oint_{C_i} a_\mu dx_\mu, \quad B_i = \oint_{C_i} b_\mu dx_\mu. \quad (1.2)$$

Given that all the matter fields carry unit a_μ or b_μ charges, the A_i and B_i should be regarded as periodic variables taking values on a circle of circumference 2π . After accounting for this periodicity, the solution of the ground state of the CS theory was found to be fourfold degenerate. The degeneracy appears exponentially fast as $L \rightarrow \infty$ provided the vison and spinon gaps remain finite. This fourfold degeneracy is viewed as an essential characterization of the Z_2 spin liquid.^{6,42}

The other phases in our phase diagrams appear when we allow one or both of s_z and s_v to vary to negative values. Then we can have phase transitions to phases in which one or both of the z_α and v_a are “condensed.” However, the precise nature of the broken symmetry, if any, is not immediately obvious in such phases, given the presence of the two gauge fields and their CS term. The purpose of this paper is to describe these phases and the associated quantum critical points. Here we note that the order parameter characterizing these states can be gleaned by carefully examining the low-energy states of \mathcal{L} on a $L \times L$ torus. As an example, consider the state where s_z is large and negative, and so a saddle point with $z_\alpha \neq 0$ is favored. By global $SU(2)$ spin symmetry, there are actually an infinite number of such saddle points along the manifold $|z_\uparrow|^2 + |z_\downarrow|^2 = \text{const}$, i.e., along S^3 , the surface of a sphere in four dimensions. The low-energy theory on an $L \times L$ torus can be expressed as a functional integral over S^3 , along with an integral over the gauge fields. We will solve

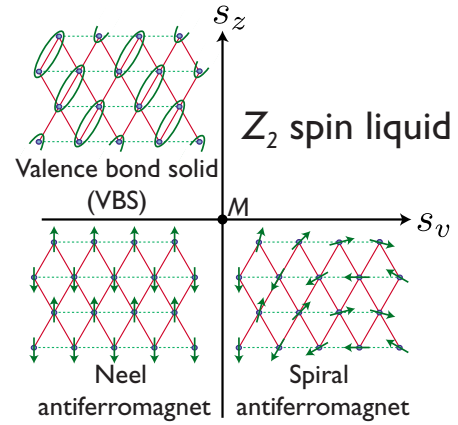


FIG. 2. (Color online) Global phase diagram for the case with $N_v=1$ and a particular model of the spinons (model BIII); a similar phase diagram appeared in Ref. 8. The Néel antiferromagnet is found in a many materials, and has ordering wave vector $\mathbf{Q} = 2\pi(1,0)$. The geometry of the VBS state coincides with that found (Refs. 20 and 21) in $\text{EtMe}_3\text{P}[\text{Pd}(\text{dmit})_2]_2$. The spiral antiferromagnet shown in the figure has an ordering wave vector $\mathbf{Q} = 2\pi(1 - \epsilon, 0)$ with $\epsilon = 1/6$, small, as expected for $J' < J$. The experimentally realized spiral state in Cs_2CuCl_4 has $J' > J$, and consequently a larger value of $\epsilon \approx 1/2$. The Z_2 spin liquid in this phase diagram is similar to that proposed in Ref. 32 to explain observations (Refs. 26–29) in $\kappa\text{-(ET)}_2\text{Cu}_2(\text{CN})_3$. The transitions have been discussed previously: (i) the CP^1 field theory for the Néel-VBS transition (Ref. 3), (ii) the $O(4)$ field theory for the spiral- Z_2 spin-liquid transition (Refs. 54–56), (iii) the mean-field theory for the spiral-Néel transition (Ref. 8), and (iv) the $O(2)$ field theory for the VBS- Z_2 spin-liquid transition (Refs. 7 and 16). All these field theories are contained in our theory in Eq. (1.1), which also describes the multicritical point M .

this quantum theory exactly, and find an “Anderson tower of states,”⁵³ with a nondegenerate ground state, and an infinite sequence of excited levels with energies $\sim 1/L^2$ above the ground-state energy. The sequence of excited levels, and their degeneracies, can be uniquely identified with the quantum mechanics of a particle moving on S^3/Z_2 , with the coordinates of the particle representing the average orientation of the order parameter across the entire torus. In other words, the primary effect of the gauge fluctuations is to reduce the order parameter characterizing the broken symmetry from S^3 to S^3/Z_2 . It was these same gauge fluctuations which were responsible for the fourfold degeneracy in the Z_2 spin liquid. The $S^3/Z_2 \cong \text{SO}(3)$ order parameter allows an immediate identification of the s_z large and negative state: this is the spiral antiferromagnet, as found in Cs_2CuCl_4 .

A related analysis for the other phases will be found in the body of the paper, allowing us to construct our phase diagrams. Here we show in Fig. 2 the phase diagram found for a case in which there is only one vison flavor, $N_v=1$, and for a particular model of the spinons—we label this theory model BIII. A mean-field phase diagram with the same phases appeared already in Ref. 8. Here we shall show that these phases follow from the very general considerations outlined above, and also provide field theories for all the transitions and the multicritical point M . It is encouraging that all the phases with broken symmetry, which descend

from the Z_2 spin liquid with $N_v=1$, correspond precisely to those which have been experimentally observed so far.

In Sec. II we will describe the phase diagram of the theory in Eq. (1.1) as an abstract field theory, without reference to any underlying antiferromagnet. The specific spinon and vison degrees of freedom of the lattice antiferromagnet, and their possible PSGs, will be identified in Sec. III. The combination of the results of Secs. II and III leads to a variety of possible phase diagrams. These are described in Sec. IV, and the quantum phase transitions are described in Sec. V. Section VI will give another semiclassical perspective on our results, which also identifies the limitations of the present U(1) CS approach. The concluding Sec. VII will make some further remarks on recent experiments.

II. PHASES OF THE DOUBLED CHERN-SIMONS THEORY

This section will discuss the phase diagram of the doubled CS theory, considered here as an abstract field theory. The interpretation of the phases in terms of the underlying antiferromagnet requires more specific knowledge of the PSGs of the spinons and visons, and these will be considered in Sec. III.

For the case where the spinons and visons are gapped, as we have already noted, we obtain the Z_2 spin liquid. The fundamental property of this theory is the fourfold degeneracy on a $L \times L$ torus, and this appears as a property of the pure doubled CS theory.^{39,43} We are now interested in moving into one of the phases where one or both of the spinons and visons are condensed and understanding the nature of the broken symmetry. As in the Z_2 spin liquid, we will do this here by examining the low-energy states of the theory on the $L \times L$ torus. We will compute the spectrum of the tower of states by Anderson⁵³ with excitation energies $\sim 1/L^2$: the spectrum of states will allow a unique identification of the ground-state manifold (GSM) associated with the broken global symmetry.

We will only consider here the case where there is a single spinon species z and a single vison species v ; the generalization to the multiple species case is straightforward. For the broken-symmetry phases, we need only consider the phases of these complex fields, and so we will write $z \sim e^{i\theta_z}$ and $v \sim e^{i\theta_v}$ where the corresponding symmetries are broken.

As a warmup, consider first the case with a single broken-U(1) symmetry, characterized by the U(1) order parameter $e^{i\theta}$, and no gauge fields. The low-energy theory of θ fluctuations is given by the action

$$\mathcal{S}_\theta = \int d^2r d\tau \left[\frac{K_1}{2} (\partial_\tau \theta)^2 + \frac{K_2}{2} (\partial_i \theta)^2 \right], \quad (2.1)$$

on an $L \times L$ torus, with θ and $\theta + 2\pi$ identified. The couplings $K_{1,2}$ are two stiffnesses characterizing the broken symmetry. Because this is a Gaussian theory, we can make the mode expansion

$$\theta(x, y, \tau) = \theta_0(\tau) + \frac{2\pi m x}{L} + \frac{2\pi n y}{L} + \frac{1}{L} \sum_{k \neq 0} a_k(\tau) e^{ik \cdot r}, \quad (2.2)$$

where n and m are fixed integers (the winding numbers), θ_0 represents the uniform fluctuation of the order parameter, and the a_k are the ‘‘spin-wave’’ normal modes. Inserting this in the action, we obtain

$$\mathcal{S}_\theta = 4\pi^2(m^2 + n^2) + \int d\tau \left[\frac{K_1 L^2}{2} (\partial_\tau \theta_0)^2 + \sum_{k \neq 0} \left(\frac{K_1}{2} (\partial_\tau a_k)^2 + \frac{K_2}{2} k^2 a_k^2 \right) \right]. \quad (2.3)$$

From this it is clear that the low-lying states have $m=n=0$. The a_k harmonic oscillators have energy $\sim k \sim 1/L$, while the θ_0 mode has energy $\sim 1/L^2$. So for the lowest states, we put all the a_k oscillators in the ground state, and we obtain a tower of states with energy

$$E_p = E_0 + \frac{p^2}{2K_1 L^2}, \quad (2.4)$$

where p is an integer, measuring the angular momentum of the θ_0 mode.

It is now useful to note that the theory \mathcal{S}_θ in Eq. (2.1) is exactly dual to U(1) gauge theory with a Maxwell term, and so the latter should have the same tower of low-energy states. Let us demonstrate this explicitly. First, we decouple the quadratic terms in Eq. (2.1) by an auxiliary current J_μ ,

$$\mathcal{S}_\theta = \int d^2r d\tau \left[\frac{J_\tau^2}{2K_1} + \frac{J_i^2}{2K_2} + iJ_\mu \partial_\mu \theta \right]. \quad (2.5)$$

Integrating over θ , we obtain the constraint $\partial_\mu J_\mu = 0$, which we solve by expressing J_μ in terms of a ‘‘dual’’ gauge field a_μ :

$$J_\mu = \frac{1}{2\pi} \epsilon_{\mu\nu\lambda} \partial_\nu a_\lambda. \quad (2.6)$$

The normalization of $1/(2\pi)$ is chosen so that periodicity of the flux variables A_i in Eq. (1.2) with period 2π is equivalent to the periodicity in the angular variable $\theta \rightarrow \theta + 2\pi$. Now inserting Eq. (2.6) into Eq. (2.5), we obtain the U(1) gauge theory dual to \mathcal{S}_θ :

$$\mathcal{S}_a = \int d^2r d\tau \left[\frac{1}{8\pi^2 K_2} (\partial_\tau a_i)^2 + \frac{1}{8\pi^2 K_1} (\partial_x a_y - \partial_y a_x)^2 \right], \quad (2.7)$$

where we have chosen the temporal gauge with $a_\tau = 0$. An important consequence of the periodicity in A_i variables is that the flux piercing the torus, $\int d^2r (\partial_x a_y - \partial_y a_x)$, must be an integer multiple of 2π . We can see this by moving the contour C_i in Eq. (1.2) across the entire length of the torus: the change in the line integral upon returning to the initial position must be an integer multiple of 2π , and this change is equal by the Stokes theorem to the flux piercing the torus. Thus the Hilbert space of \mathcal{S}_a breaks apart into distinct sectors

with total flux $2\pi p$, where p is an integer. Within each sector, the ground state has zero photons (which are the dual of the spin waves), and has $\langle \partial_x a_y - \partial_y a_x \rangle = (2\pi p)/L^2$. So the lowest-energy state in each sector is

$$E_p = E_0 + \frac{L^2}{8\pi^2 K_1} \left(\frac{2\pi p}{L^2} \right)^2 = E_0 + \frac{p^2}{2K_1 L^2}, \quad (2.8)$$

which is the same as the spectrum of S_θ in Eq. (2.4). This verifies the equivalence of Eqs. (2.1) and (2.7).

With these preliminaries out of the way, let us return to our doubled CS theory with one spinon and one vison. Consider the phase where the spinon is condensed and the vison is gapped, so $s_v \gg 0$ and $s_z \ll 0$. Here we can simply integrate out the vison, and are left with the following low-energy theory for θ_z and the U(1) gauge fields:

$$\mathcal{S}_z = \int d^2 r d\tau \left[\frac{K_1}{2} (\partial_\tau \theta_z - a_\tau)^2 + \frac{K_2}{2} (\partial_i \theta_z + a_i)^2 + \frac{ik}{2\pi} a_\mu \epsilon_{\mu\nu\lambda} \partial_\nu b_\lambda \right]. \quad (2.9)$$

We can always choose the gauge $\theta_z=0$ (and $A_z=0$). In this gauge, the integral over a_μ is an ordinary Gaussian. Performing this integral, we obtain the action

$$\mathcal{S}_z = \int d^2 r d\tau \left[\frac{k^2}{8\pi^2 K_2} (\partial_\tau b_t)^2 + \frac{k^2}{8\pi^2 K_1} (\partial_x b_y - \partial_y b_x)^2 \right]. \quad (2.10)$$

Comparing this with the spectrum of \mathcal{S}_a in Eq. (2.8), we obtain the low-lying states

$$E_p = E_0 + \frac{k^2 p^2}{2K_1 L^2}. \quad (2.11)$$

This shows that the theory \mathcal{S}_z in Eq. (2.9) is equivalent to the U(1) scalar theory in Eq. (2.1) but with the periodicity $\theta \equiv \theta + 2\pi/k$. In other words, the GSM of this phase has been modified by the gauge fluctuations from S^1 to S^1/Z_k . Alternatively stated, the broken symmetry of the ground state is associated with distinct values of the composite field z^k .

It is useful to have another perspective on the above result by an alternative analysis of the theory \mathcal{S}_z in Eq. (2.9). This analysis begins by “undualizing” the gauge field b_μ into a dual scalar θ_b . For this we introduce, as in Eq. (2.6), the current $J_\mu^b = \epsilon_{\mu\nu\lambda} \partial_\nu b_\lambda / (2\pi)$ and impose the constraint $\partial_\mu J_\mu^b = 0$ by a Lagrange multiplier θ_b ; this modifies \mathcal{S}_z in Eq. (2.9) to

$$\mathcal{S}_z = \int d^2 r d\tau \left[\frac{K_1}{2} (\partial_\tau \theta_z - a_\tau)^2 + \frac{K_2}{2} (\partial_i \theta_z + a_i)^2 + iJ_\mu^b (ka_\mu - \partial_\mu \theta_b) + \frac{J_\mu^b J_\mu^b}{2\tilde{K}} \right]. \quad (2.12)$$

The last term is a useful regularization, and the original theory in Eq. (2.9) is obtained in the limit $\tilde{K} \rightarrow \infty$. Now we perform the integral over J_μ^b and obtain the theory

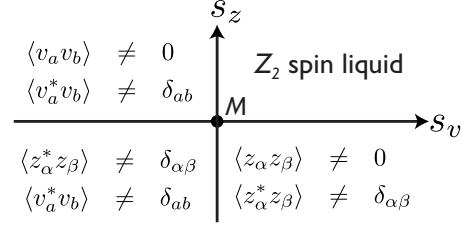


FIG. 3. Schematic phase diagram of the doubled CS theory in Eq. (1.1) for $k=2$. All nonzero order parameters which characterize the broken symmetry in each phase are shown.

$$\mathcal{S}_z = \int d^2 r d\tau \left[\frac{K_1}{2} (\partial_\tau \theta_z - a_\tau)^2 + \frac{K_2}{2} (\partial_i \theta_z + a_i)^2 + \frac{\tilde{K}}{2} (ka_\mu - \partial_\mu \theta_b)^2 \right]. \quad (2.13)$$

In the limit $\tilde{K} \rightarrow \infty$, we see that we must have $a_\mu = (1/k) \partial_\mu \theta_b$. However, θ_b is a variable periodic under $\theta_b \rightarrow \theta_b + 2\pi$, and hence the periodic flux variables A_i in Eq. (1.2) can only take the values

$$A_i = \frac{2\pi p_i}{k}, \quad (2.14)$$

where the p_i are integers. In other words, U(1) gauge field a_μ has been reduced to a Z_k gauge field. Thus $e^{ik\theta} \sim z^k$ is gauge invariant, and this explains our results above on the distinct values of z^k identifying distinct ground states.

We have now completed our discussion of the state where the spinon is condensed and the vison is gapped ($s_v \gg 0$ and $s_z \ll 0$). Clearly, the complementary phase where the vison is condensed and the spinon is gapped ($s_v \ll 0$ and $s_z \gg 0$) is amenable to a parallel treatment, with complementary results and a v^k order parameter.

Finally, let us consider the case where both the visons and spinons are condensed, $s_v \ll 0$ and $s_z \ll 0$. In this case, we can see in the gauges $\theta_z=0$ and $\theta_b=0$ that both fields a_μ and b_μ are fully gapped. So there is a unique ground state, and no other excited states whose energy vanishes as $L \rightarrow \infty$.

We can now generalize these results to the cases with multiple flavors of visons and spinons, and the results are summarized in Fig. 3 for $k=2$. The flavor indices simply tag along for the order parameters involving a k -fold composites of spinons or visons, which are invariant under the Z_k gauge transformations. However, there are now also additional gauge-neutral order parameters possible, such as $z_\alpha^* z_\beta$, which were absent for the single-flavor case, because they were not associated with any broken symmetry. Armed with the results in Fig. 3 and with knowledge of the microscopic PSGs of the spinons and visons (which are described next in Sec. III), we can easily deduce the physical characteristics of the phases of a variety of antiferromagnets.

III. SPINONS AND VISONS

A rich variety of spinon and vison operators can be defined for $S=1/2$ antiferromagnets on the lattice in Fig. 1, and

we shall not attempt any complete classification. Clearly, the choice depends sensitively on the details of the microscopic Hamiltonian. However, in previous semiclassical analyses, a few natural choices have emerged for different limiting values of J'/J . We will describe these below and show how they can fit together in a doubled CS theory such as Eq. (1.1).

The essential characteristics of the spinons and visons will be their transformations under the symmetry operations of the underlying spin model. These symmetries are the lattice translations T_1 and T_2 , the lattice reflections P_x and P_y , and time reversal T :

$$\begin{aligned} T_1: (x,y) &\rightarrow (x+1,y), \\ T_2: (x,y) &\rightarrow (x+1/2,y+\sqrt{3}/2), \\ P_x: (x,y) &\rightarrow (-x,y), \\ P_y: (x,y) &\rightarrow (x,-y), \\ T: t &\rightarrow -t. \end{aligned} \quad (3.1)$$

Spin rotation is also a symmetry and is easily implemented by contracting the spinor indices. Sections III A and III B will consider the PSGs of spinons and visons in turn.

A. Spinons

One natural model of spinons appears upon describing the spiral ground state of the triangular lattice antiferromagnet in terms of Schwinger bosons. So we write the spin operator on the lattice sites as $\vec{S} = b^\dagger \vec{\sigma} b / 2$, where $\vec{\sigma}$ are the Pauli matrices. For the Schwinger bosons we make the following low-energy expansion⁵⁷ in terms of the spinon fields z_α :

$$b_\alpha \sim z_\alpha \exp(i\mathbf{Q} \cdot \mathbf{r}/2) + i\epsilon_{\alpha\beta\gamma} z_\beta^* \exp(-i\mathbf{Q} \cdot \mathbf{r}/2). \quad (3.2)$$

From this parametrization we can then deduce the following expression for the spin operators:

$$\begin{aligned} \vec{S} &= \vec{n}_1 \cos(\mathbf{Q} \cdot \mathbf{r}) + \vec{n}_2 \sin(\mathbf{Q} \cdot \mathbf{r}), \\ \vec{n}_1 &= \text{Re}[z^t \sigma^y \vec{\sigma} z], \quad \vec{n}_2 = \text{Im}[z^t \sigma^y \vec{\sigma} z], \\ \vec{n}_3 &= \vec{n}_1 \times \vec{n}_2 = z^\dagger \vec{\sigma} z. \end{aligned} \quad (3.3)$$

We observe that \mathbf{Q} is the ordering wave vector of the spiral. So for $J' \approx J$, we expect $\mathbf{Q} \approx (2\pi/3, 0)$. For Cs_2CuCl_4 , which has $J' \approx 3J$, we have $\mathbf{Q} \approx (\pi, 0)$. Finally, in the square lattice limit, $J' \ll J$, we have $\mathbf{Q} \approx (2\pi, 0)$. Thus we expect \mathbf{Q} to increase monotonically from $(\pi, 0)$ to $(2\pi, 0)$ with decreasing J'/J . Also note that $\vec{n}_{1,2,3}$ are three mutually orthogonal vectors.

The parametrization in Eq. (3.3) allows us to deduce the PSG of the z_α . These z_α spinons will couple minimally to the a_μ gauge field, and so there is a natural implied PSG for the a_μ . We call the resulting PSG of spinons as model A,

Spinons, model A:

$$T_1: z \rightarrow e^{iQx/2} z, \quad a_\mu \rightarrow a_\mu,$$

$$T_2: z \rightarrow e^{iQy/4} z, \quad a_\mu \rightarrow a_\mu,$$

$$P_x: z_\alpha \rightarrow \epsilon_{\alpha\beta\gamma} z_\beta^*, \quad a_x \rightarrow a_x, \quad a_y \rightarrow -a_y, \quad a_t \rightarrow -a_t,$$

$$P_y: z \rightarrow z, \quad a_x \rightarrow a_x, \quad a_y \rightarrow -a_y, \quad a_t \rightarrow a_t,$$

$$T: z \rightarrow iz^*, \quad a_\mu \rightarrow a_\mu. \quad (3.4)$$

We note that under this model A PSG, $\vec{n}_{1,2}$ are odd under time reversal, while \vec{n}_3 is even. From this, and the representation in Eq. (3.3), we deduce that \vec{n}_3 is a spin nematic order parameter.

The model A spinons are natural for $J' \geq J$, where the spiral order is likely to be present. However as we approach the square lattice limit with $J' \rightarrow 0$, there is a finite range of small $J' < J$ over which we expect that \mathbf{Q} is pinned exactly at $(2\pi, 0)$, and we have the conventional two-sublattice Néel order appropriate for the square lattice. In this case $\sin(\mathbf{Q} \cdot \mathbf{r}) = 0$ identically, and $\cos(\mathbf{Q} \cdot \mathbf{r}) = \cos(2\pi x) = (-1)^{2x}$. In this limit, we can define another model of spinons which appeared in previous theories of square lattice antiferromagnets.^{1,2} We map $z_\alpha \rightarrow (z_\alpha + i\epsilon_{\alpha\beta\gamma} z_\beta^*) / \sqrt{2}$ and then find that Eq. (3.3) is replaced by

$$\vec{S} = \vec{m}_1 (-1)^{2x}, \quad \vec{m}_1 = z^\dagger \vec{\sigma} z, \quad (3.5)$$

A significant difference from Eq. (3.3) is that now the U(1) gauge invariance associated with a_μ is explicit, because representation (3.5) is invariant under the gauge transformation $z_\alpha \rightarrow z_\alpha e^{i\theta}$. We label these spinons model B, and they also have mappings under the square lattice space group, which we can deduce from Eq. (3.5) to be

Spinons, model B:

$$T_1: z \rightarrow -z, \quad a_\mu \rightarrow a_\mu,$$

$$T_2: z_\alpha \rightarrow -\epsilon_{\alpha\beta\gamma} z_\beta^*, \quad a_\mu \rightarrow -a_\mu,$$

$$P_x: z \rightarrow iz, \quad a_x \rightarrow -a_x, \quad a_y \rightarrow a_y, \quad a_t \rightarrow a_t,$$

$$P_y: z \rightarrow z, \quad a_x \rightarrow a_x, \quad a_y \rightarrow -a_y, \quad a_t \rightarrow a_t,$$

$$T: z_\alpha \rightarrow \epsilon_{\alpha\beta\gamma} z_\beta, \quad a_\mu \rightarrow -a_\mu. \quad (3.6)$$

It is now clear that under the model B PSG, \vec{m}_1 is odd under time reversal. In the state where the spinons are condensed and the visons are gapped, we see from Fig. 3 that we also have two additional vectors in spin space which characterize the broken symmetry in the ground state (analogous to the three vectors found in model A):

$$\vec{m}_2 + i\vec{m}_3 = z^t \sigma^y \vec{\sigma} z. \quad (3.7)$$

These vectors do not appear in the present expression for the spin operator in Eq. (3.5), and so their physical interpretation is not yet clear. Let us, therefore, compute the PSG of these vectors,

Model B:

$$T_1: \vec{m}_{2,3} \rightarrow \vec{m}_{2,3},$$

$$T_2: \vec{m}_2 \rightarrow \vec{m}_2, \quad \vec{m}_3 \rightarrow -\vec{m}_3,$$

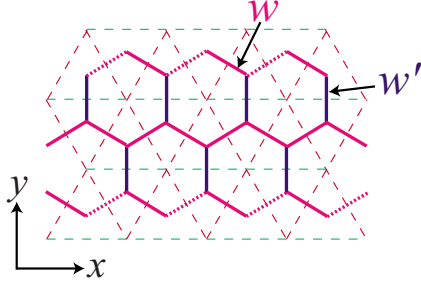


FIG. 4. (Color online) The dual Ising model describing the vison dynamics in the dual honeycomb lattice. All the vertical bonds have hopping amplitude w' ; all the other bonds have hopping amplitude w . Note that a small J'/J implies a large w'/w , and vice versa. Besides the lattice anisotropy, there is a π flux through every hexagon, which frustrates the vison kinetics. This flux is implemented by changing the sign of the dotted w bonds.

$$\begin{aligned}
 P_x: \vec{m}_{2,3} &\rightarrow -\vec{m}_{2,3}, \\
 P_y: \vec{m}_{2,3} &\rightarrow \vec{m}_{2,3}, \\
 T: \vec{m}_2 &\rightarrow \vec{m}_2, \quad \vec{m}_3 \rightarrow -\vec{m}_3.
 \end{aligned} \quad (3.8)$$

From these properties it is evident that we can identify \vec{m}_2 as the central axis (in spin space) about which the spins are precessing in the spiral antiferromagnet shown in Fig. 2. We will present a more detailed analysis in Sec. IV D which shows how the spiral state emerges for model B spinons. This identification is also consistent with the analysis of this phase in Ref. 8, where the spiral phase was induced by the condensation of a charge 2 Higgs scalar—the vison is dual to this scalar, and the gapping of the vison is equivalent to the condensation of the Higgs scalar.

B. Visions

In the simplest models of visons,^{7,16,36} we take real particles hopping on the sites of the dual lattice, subject to a flux of π around every site of the direct lattice. In other words, the vison is the Ising field of an Ising model on the dual lattice, with exchange couplings chosen so that every plaquette surrounding a direct lattice site is frustrated. For the antiferromagnet on the lattice in Fig. 1, the Ising model resides on the dual lattice shown in Fig. 4. Because of the dual relation between the couplings of the antiferromagnet and the model of the visons, we expect that w'/w decreases as J'/J increases.

It is a relatively straightforward matter to obtain the spectrum of such a particle moving on the lattice in Fig. 4. Because the kinetics of the vison is frustrated by the background spinon charge on every site, the product of the hopping amplitudes on the six links around each hexagon is -1 . We are free to choose one of the links to be negative, and our convention is shown in Fig. 4. The spectrum has multiple minima in the Brillouin zone, and we introduce a real vison field for each such minimum in the spectrum. This procedure parallels that carried out in obtaining the multiple vortex flavors in Refs. 58 and 59, but with modification that we are

considering real vison fields and not complex vortex fields.

For the general set of parameters for the lattice in Fig. 4, we find that there are either four or two minima of the vison dispersion lattice in the Brillouin zone. The four minima occur near $J' \approx J$, and so are appropriate for the triangular lattice limit; indeed for $J' = J$ these minima coincide with those found by Moessner and Sondhi.¹⁶ For J'/J small (w'/w large), near the square lattice limit, we find only two minima.

Let us begin by considering the four-minima case. These are at momenta of the form

$$\begin{aligned}
 \mathbf{q}_1 &= (q_{1x}, \pi/2), \\
 \mathbf{q}_2 &= (\pi - q_{1x}, \pi/2), \\
 \mathbf{q}_3 &= (-q_{1x}, -\pi/2), \\
 \mathbf{q}_4 &= (q_{1x} - \pi, -\pi/2).
 \end{aligned} \quad (3.9)$$

There are two choices to combine these four real minima to two complex minima, which will then correspond to the complex vison fields v_a , with $a=1, 2$. The first choice, which we call model I, is

$$\begin{aligned}
 v_1: \mathbf{q}_1 &= (q_{1x}, \pi/2), \\
 v_2: \mathbf{q}_2 &= (\pi - q_{1x}, \pi/2), \\
 v_1^*: \mathbf{q}_3 &= (-q_{1x}, -\pi/2), \\
 v_2^*: \mathbf{q}_4 &= (q_{1x} - \pi, -\pi/2),
 \end{aligned} \quad (3.10)$$

while model II is

$$\begin{aligned}
 v_1: \mathbf{q}_1 &= (q_{1x}, \pi/2), \\
 v_2^*: \mathbf{q}_2 &= (\pi - q_{1x}, \pi/2), \\
 v_1^*: \mathbf{q}_3 &= (-q_{1x}, -\pi/2), \\
 v_2: \mathbf{q}_4 &= (q_{1x} - \pi, -\pi/2).
 \end{aligned} \quad (3.11)$$

These two choices lead to two models for the vison PSGs,

Visons, model I:

$$\begin{aligned}
 T_1: v_1 &\rightarrow e^{iq_{1x}}v_1, \quad v_2 \rightarrow e^{i\pi - iq_{1x}}v_2, \quad b_\mu \rightarrow b_\mu, \\
 T_2: v_1 &\rightarrow e^{i\theta}v_2^*, \quad v_2 \rightarrow -ie^{-i\theta}v_1^*, \quad b_\mu \rightarrow -b_\mu, \\
 P_x: v_1 &\rightarrow e^{-i\gamma}v_1^*, \quad v_2 \rightarrow -e^{i\gamma}v_2^*, \quad b_x \rightarrow b_x, \\
 & \quad b_y \rightarrow -b_y, \quad b_t \rightarrow -b_t, \\
 P_y: v_1 &\rightarrow v_2^*, \quad v_2 \rightarrow v_1^*, \quad b_x \rightarrow -b_x, \quad b_y \rightarrow b_y, \\
 & \quad b_t \rightarrow -b_t, \\
 T: v_a &\rightarrow v_a^*, \quad b_\mu \rightarrow b_\mu,
 \end{aligned} \quad (3.12)$$

where γ and θ are two incommensurate angles.

The second model for the vison PSG is

Visons, model II:

$$T_1: v_1 \rightarrow e^{iq_1 x} v_1, \quad v_2 \rightarrow e^{-i\pi+iq_1 x} v_2, \quad b_\mu \rightarrow b_\mu,$$

$$T_2: v_1 \rightarrow e^{i\theta} v_2, \quad v_2 \rightarrow i e^{i\theta} v_1, \quad b_\mu \rightarrow b_\mu,$$

$$P_x: v_1 \rightarrow e^{-i\gamma} v_1^*, \quad v_2 \rightarrow -e^{-i\gamma} v_2^*, \quad b_x \rightarrow b_x, \\ b_y \rightarrow -b_y, \quad b_t \rightarrow -b_t,$$

$$P_y: v_1 \rightarrow v_2, \quad v_2 \rightarrow v_1, \quad b_x \rightarrow b_x, \quad b_y \rightarrow -b_y, \quad b_t \rightarrow b_t,$$

$$T: v_a \rightarrow v_a^*, \quad b_\mu \rightarrow b_\mu, \quad (3.13)$$

where again γ and θ are two incommensurate angles when the lattice is distorted. For an isotropic triangular lattice, $\theta = -\pi/12$ and $\gamma = \pi/6$, and they will continuously evolve to vison model III by tuning the distortion of the lattice.

Finally, let us move to the case where the four minima in the vison band merge to two. In model I, v_1 and v_2 merge together, while in model II v_1 and v_2^* merge together. But v_1 and v_2^* carry opposite gauge charges in the CS theory, and so this merger violates the gauge invariance. So if we want to evolve smoothly from four minima to two minima, we have to take model I.

After the merger, the two minima are located at $(\pi/2, \pi/2)$ and $(-\pi/2, -\pi/2)$. So we have just to use one component complex vison v , and its PSG leads to

Visons, model III:

$$T_1: v \rightarrow iv, \quad b_\mu \rightarrow b_\mu,$$

$$T_2: v \rightarrow -e^{3\pi i/4} v^*, \quad b_\mu \rightarrow -b_\mu,$$

$$P_x: v \rightarrow -iv^*, \quad b_x \rightarrow b_x, \quad b_y \rightarrow -b_y, \quad b_t \rightarrow -b_t,$$

$$P_y: v \rightarrow v^*, \quad b_x \rightarrow -b_x, \quad b_y \rightarrow b_y, \quad b_t \rightarrow -b_t,$$

$$T: v \rightarrow v^*, \quad b_\mu \rightarrow -b_\mu. \quad (3.14)$$

Finally, we consider the nature of the vison order parameters $v_a v_b$ and $v_a^* v_b$ which appear in the phases in Fig. 3. The simplest case is model III, with only one complex vison v , in which case the only nontrivial order parameter is v^2 . From the PSG, we see that v^2 is the square lattice VBS order parameter, associated with the VBS state shown in Fig. 2. Using the definitions $V_{\bar{x}\bar{y}}$ for this order parameter in Ref. 3, we have $V_{\bar{x}} \sim \cos(\phi + \pi/4)$ and $V_{\bar{y}} \sim \cos(\phi - \pi/4)$, where $v^2 = \exp(i\phi)$. Here (and henceforth), the axes \bar{x} and \bar{y} refer to the principle axes of the ‘‘square’’ lattice formed by the J bonds in Fig. 1.

The vison order parameters for the other models also describe VBS orders but of a different nature. The vison operator v_a is subject to a Z_2 gauge invariance. Therefore the physical VBS order parameter should always be bilinear in v_a . There are in total 15 independent bilinear of v_a , and the detailed VBS pattern drive by vison proliferation depends on the Hamiltonian of visons, which will be discussed in Sec. IV.

TABLE I. Transformation of the mutual Chern-Simons term under the space-group operations for the various theories. The CS term changes its overall sign, as indicated.

	BI and BIII	AI and AIII	AII	BII
T_1	+	+	+	+
T_2	+	-	+	-
P_x	+	-	-	+
P_y	+	+	-	-
T	+	-	-	+

IV. PHASE DIAGRAMS

Now we turn to the crucial question of combining the spinon and vison PSGs in Sec. III into consistent theories of the form in Eq. (1.1). We will denote the resulting theories by an obvious notation; i.e., the theory BIII has spinons under model B and visons under model III.

In principle, there are now six possible theories, AI, AII, AIII, BI, BII, and BIII, and associated phase diagrams. To establish the consistency of these theories, we have to examine the transformation of the CS term under the respective spinon and vison PSGs. The results of such an analysis are summarized in Table I for all theories. We see that under theories BI and BIII the Chern-Simons term is strictly invariant, and so these theories are clearly consistent. For the remaining theories, the overall form of the CS term remains invariant, but some of the transformations do lead to a change in sign of the CS term. However, the role of the CS term here for $k=2$ is only to implement a mutual semionic phase of π , and this is invariant under the sign change. Equivalently, we are free to define the vison at momentum \mathbf{Q} to be either v or v^* , which means that in the system there should be particle-hole symmetry of vison; i.e., on average the spinons see zero flux. This particle-hole symmetry corresponds to the free choice of the sign of gauge charge of vison, and leads to the freedom of the sign of the mutual CS term.

A. Model AI

The Lagrangian should be invariant under all the symmetry and PSG transformations, which in general takes the form

$$\mathcal{L} = \sum_{\alpha=1}^2 \{ |(\partial_\mu - ia_\mu) z_\alpha|^2 + s_z |z_\alpha|^2 \} \\ + \sum_{a=1}^2 \{ |(\partial_\mu - ib_\mu) v_a|^2 + s_v |v_a|^2 \} + \frac{ik}{2\pi} \epsilon_{\mu\nu\lambda} a_\mu \partial_\nu b_\lambda \\ + u_z \left(\sum_{\alpha=1}^2 |z_\alpha|^2 \right)^2 + u_v \left(\sum_{a=1}^2 |v_a|^2 \right)^2 + g |v_1|^2 |v_2|^2 + \dots \quad (4.1)$$

Let us first identify all the symmetries of this Lagrangian. The U(1) gauge symmetries associated with gauge field a_μ and b_μ , correspond to two global U(1) symmetries U(1)_a

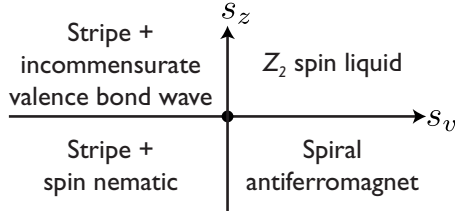


FIG. 5. Phase diagram of model AI with $g > 0$. The stripe order is illustrated in Fig. 7, while the spiral antiferromagnet is as in Fig. 2.

$\times U(1)_b$ in the dual picture, which lead to the conservation of gauge fluxes. Through the mutual CS term, the gauge flux of a_μ is attached with the vison number, and the gauge flux of b_μ is attached with the spinon number. On top of the $U(1)$ gauge symmetries, the global symmetry of this Lagrangian to the fourth order of z_α and v_a is $SU(2)_{\text{spin}} \times U(1) \times Z_2$. The $U(1)$ symmetry corresponds to the $U(1)$ transformation on vison bilinear $v_1^* v_2$; the Z_2 symmetry corresponds to interchanging v_1 and v_2 , which physically can be understood as the reflection symmetry P_y . If the lattice is an undistorted triangular lattice, $g=0$, and the vison doublet enjoys an enlarged $SU(2)$ flavor symmetry in this mutual CS theory [or an $O(4)$ symmetry in a theory with only vison]. The ellipses in Eq. (4.1) include terms no less than sixth order of v_a , which may introduce higher-order anisotropy. In the distorted triangular lattice, the lowest-order term which breaks the symmetries in Eq. (4.1) is at the eighth order:

$$\mathcal{L}_8 = g_8 (v_1 v_2)^4 + \text{H.c.} \quad (4.2)$$

In the undistorted lattice, the lowest-order symmetry-breaking term is at the sixth order. If only the terms below fourth order are considered, we can minimize the Lagrangian in Eq. (4.1) with tuning parameters s_z and s_v , and obtain the phase diagrams in Figs. 5 and 6, with the phases described in Secs. IV A 1 and IV A 3.

1. Z_2 spin-liquid and spiral phases

The phase with both the spinons and visons gapped out ($s_z > 0, s_v > 0$) is the Z_2 spin liquid, as was discussed in Secs. I and II, has fourfold topological degeneracy on a compact torus. The phase with visons gapped and spinons condensed ($s_v > 0, s_z < 0$), is the incommensurate spin spiral state, with wave vector \mathbf{Q} . With the vison gapped, the gauge field b_μ is in the photon phase, and so the CS term ‘‘Higgses’’ out the gauge field a_μ . Or more precisely, for $k=2$, one gauge flux of b_μ carries two gauge charges of a_μ . Therefore the photon

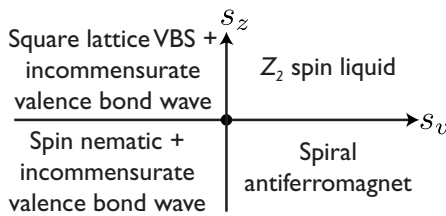


FIG. 6. Phase diagram of model AI with $g < 0$. The square lattice VBS state is as illustrated in Fig. 2.

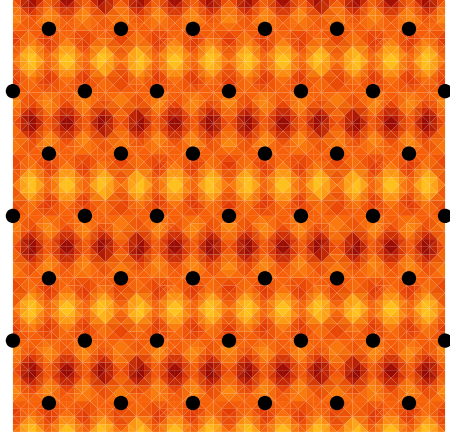


FIG. 7. (Color online) Illustration of the Z_2 stripe order. This can be viewed as a bond density wave, with alternating signs on successive rows of bonds.

phase of b_μ , which is the superfluid phase of gauge flux, breaks the $U(1)$ gauge invariance of a_μ to Z_2 , as was discussed in Sec. II. As also noted in Sec. II, this implies that the GSM of the spinon condensate is S^3/Z_2 , and this is the GSM of the spiral spin state. Another way to understand this phase is that, because the vison number is attached with the flux number of a_μ through the mutual CS term, in the Mott insulator phase of vison the photon of a_μ is gapped out, while b_μ is in the photon phase. The global symmetry $U(1)_b$ becomes the global $U(1)$ symmetry of the spinon z_α , which according to the PSG in Eq. (3.4) corresponds to the physical translation transformation.

2. Vison condensate with $s_v < 0$ and $s_z > 0$

The nature of the phase with spinon gapped and vison condensed depends on the sign of g in Eq. (4.1). With the spinon gapped, the $U(1)$ gauge field b_μ is broken down to Z_2 gauge field. Integrating out the remnant Z_2 gauge field, the vison v_a enjoys a $U(1) \times U(1) \times Z_2$ symmetry. The two $U(1)$'s correspond to the global symmetry of two flavors of visons respectively, and the Z_2 symmetry corresponds to the interchange symmetry between v_1 and v_2 . With $g > 0$, the vison condensate breaks the $U(1) \times U(1) \times Z_2$ symmetry to $U(1)$ symmetry; i.e., only one flavor of v_a condenses. Let us assume z_1 condenses, and z_2 remains gapped. The GSM of the vison condensate is $S^1 \times Z_2$. The Z_2 degeneracy is described by the Ising order parameter $v^\dagger \sigma^z v$, which corresponds to the stripe order depicted in Fig. 7. The S^1 in the GSM is described by the order parameter v_1^2 , which corresponds to an incommensurate valence-bond density wave along the x direction with wave vector $(2q_{1x}, \pi)$, and meanwhile breaks the Ising symmetry of interchanging v_1 and v_2 , or the reflection symmetry P_y . The continuous symmetry $U(1)$ transformation of v_1 which has been broken by this valence-bond density wave is the translation along \hat{x} . Because v_1 carries an incommensurate momentum, the full Lagrangian in Eq. (4.1) with all the higher-order perturbation should preserve this global $U(1)$ symmetry, and the GSM $S^1 \times Z_2$ is not broken down to smaller manifolds. For instance, the eighth-order term \mathcal{L}_8 violates the vison numbers

of both v_1 and v_2 ; in the phase with only v_1 condensed, \mathcal{L}_8 is suppressed.

If $g < 0$, the vison condensate breaks its global symmetry to Z_2 ; i.e., both v_1 and v_2 condense with equal stiffness. The GSM is $S^1 \times S^1$ if there are no more symmetry-breaking terms. The two S^1 's correspond to two U(1) order parameters $v_1 v_2$ and $v_1^* v_2^*$, respectively. The U(1) symmetry of $v_1^* v_2^*$ is preserved by the full Lagrangian, while the U(1) symmetry of $v_1 v_2$ is broken by the eighth-order term \mathcal{L}_8 in Eq. (4.2). This term breaks the U(1) symmetry of $v_1 v_2$ to Z_4 symmetry. Actually, the order parameter $v_1 v_2$ corresponds to the Z_4 degeneracy of the four VBS states, which are smoothly connected to the fourfold-degenerate VBS states in the square lattice limit with $J' \sim 0$. Using the square lattice coordinates, the VBS order parameters are

$$\begin{aligned} V_{\bar{x}} &\sim v_1 v_2 \exp(i\pi/4) + v_1^* v_2^* \exp(-i\pi/4), \\ V_{\bar{y}} &\sim v_1 v_2 \exp(-i\pi/4) + v_1^* v_2^* \exp(i\pi/4). \end{aligned} \quad (4.3)$$

The square lattice VBS order is selected when $g_8 > 0$; otherwise the fourfold-degenerate plaquette state is favored. On top of this commensurate VBS order, an incommensurate valence-bond density wave corresponding to $v_1^* v_2$ is also present, with wave vector $(\pi - 2q_{1x}, 0)$.

3. Phase with both spinons and visons condensed ($s_z < 0$ and $s_v < 0$)

The most interesting phase is the phase with both spinons and visons condensed. In this phase, the physical order parameter should be the U(1) gauge-invariant bilinears of z_α and v_α , as discussed in Sec. II. The spin order parameter is the nematic vector $\vec{n}_3 \sim z^\dagger \sigma^a z$. The VBS pattern, depending on the sign of g , is either the Z_2 order parameter $v^\dagger \sigma^x v$ or the incommensurate valence-bond density wave $v_1^* v_2$. Note, however, that the commensurate VBS order parameters $V_{\bar{x}}$ and $V_{\bar{y}}$ vanish because they are not gauge invariant. Another way of understanding the vanishing of $V_{\bar{x}}$ and $V_{\bar{y}}$ is as follows: when the spinon z_α is still condensed, the flux of a_μ is in the Mott insulator phase. Because the flux number of a_μ is attached to the vison number through the mutual CS term, any order parameter violating the vison number conservation should not condense. The GSM of this phase is either $S_{\text{spin}}^2 \times Z_2$ ($g > 0$) or $S_{\text{spin}}^2 \times S^1$ ($g < 0$). Furthermore, these GSMs are not lifted by any higher-order term in Lagrangian equation (4.1).

Also note that \mathcal{L}_8 in Eq. (4.2) violates the gauge symmetry of b_μ . In the condensate of visons, L_8 confines the fluxes of b_μ , and hence the spinon excitation z_α is also confined, which is consistent with the intuitive understanding of VBS states.

B. Model AII

The phase diagram of this model is very similar to that in Sec. IV A, model AI. The only difference is that we now replace v_2 with v_2^* . So the spiral spin-density wave, the Z_2 spin liquid, and the VBS order are the same as in model AI. The commensurate VBS order parameter is now represented as

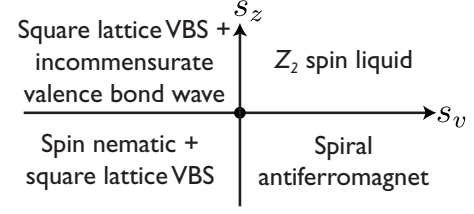


FIG. 8. Phase diagram of model AII with $g < 0$. The phase diagram of model AII with $g > 0$ is the same as that for model AI with $g > 0$.

$$V_{\bar{x}} \sim v_1 v_2^* \exp(i\pi/4) + v_1^* v_2 \exp(-i\pi/4),$$

$$V_{\bar{y}} \sim v_1 v_2^* \exp(-i\pi/4) + v_1^* v_2 \exp(i\pi/4). \quad (4.4)$$

In addition the incommensurate valence-bond wave is represented by $v_1 v_2$.

In model AII, the VBS pattern with both spinons and visons condensed is different from model AI. Because in this phase all the physical order parameters should be U(1) gauge invariant, the VBS order parameter is either the Z_2 symmetry-breaking $v^\dagger \sigma^x v$, or the Z_4 symmetry-breaking $V_{\bar{x}}$ and $V_{\bar{y}}$ depending on the sign of g . The GSM is $S_{\text{spin}}^2 \times Z_2$ ($g > 0$) or $S_{\text{spin}}^2 \times Z_4$ ($g < 0$). The phase diagram is shown in Fig. 8.

C. Model AIII

In this model there is only one complex vison. The Z_2 spin liquid and the spiral spin state are the same as in the two previous models. The vison condensate induces the fourfold-degenerate VBS order, with order parameters $V_{\bar{x}} \sim v^2 \exp(i\pi/4) + \text{H.c.}$ and $V_{\bar{y}} \sim v^2 \exp(-i\pi/4) + \text{H.c.}$ However, one can no longer write down a U(1) gauge-invariant order parameter in terms of v . Therefore the phase with both spinons and visons condensed has only the nematic order \vec{n}_3 , and no other lattice symmetry breaking. The phase diagram is shown in Fig. 9.

If the parameter t'/t is tuned, the four vison minima will merge to two vison minima; i.e., the two complex visons become one complex vison. Therefore by tuning t'/t , model AIII can be connected to model AI.

D. Models BI, BII, and BIII

These models are similar to models AI, AII, and AIII. The main difference is that in the phase with both spinons and visons condensed, the spin order is the collinear Néel order,

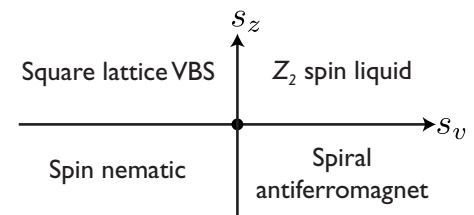


FIG. 9. Phase diagram of model AIII.

in place of the spin nematic order parameter. The phase diagram for model BIII was shown in Fig. 2.

We now discuss in some detail how the spiral order emerges in model B, as this is not evident from the underlying spin representation in Eq. (3.5). If we use only the constraints imposed by the model B PSG in Eq. (3.6), then the Lagrangian of the spinons allows an additional linear spatial derivative term in the Lagrangian of spinon of

$$\mathcal{L}_x \sim \epsilon_{\alpha\beta\gamma\alpha} \nabla_x z_\beta + \text{H.c.} \quad (4.5)$$

The term \mathcal{L}_x violates the enlarged U(1) gauge invariance of the mutual CS Lagrangian discussed below Eq. (3.5). The mutual CS term will bind this term with the monopole operator of b_μ , which creates $2\pi b_\mu$ gauge flux. We denote this monopole operator by \mathcal{M}_b , then in the U(1) gauge-invariant formalism \mathcal{L}_x reads

$$\mathcal{L}_x \sim \mathcal{M}_b \epsilon_{\alpha\beta\gamma\alpha} \nabla_x z_\beta + \text{H.c.} \quad (4.6)$$

In the phase with both spinons and visons condensed, the term \mathcal{L}_x is suppressed because of the conservation of the flux of b_μ which is attached to the spinon number of z_α . However, once the visons are gapped, the monopoles \mathcal{M}_b condense and \mathcal{L}_x becomes relevant. Due to its linear derivative of x , \mathcal{L}_x will drive the system into an incommensurate spiral state with wave vector along \hat{x} axis, as has been described in Ref. 8. The size of the incommensurate wave vector increases linearly with $\langle \mathcal{M}_b \rangle \sim \sqrt{\rho_b}$, where ρ_b is the stiffness of the b_μ flux condensate, which is proportional to the gap of vison.

V. QUANTUM PHASE TRANSITIONS

There are many phase transitions involved in the phase diagrams discussed in Sec. IV. We will study them in the same manner as in Sec. IV.

Before turning to the individual cases, it is useful to discuss an alternative form of the mutual CS theories [Eq. (1.1)]. For many of the vison models, it is possible to^{60,61} undualize the vison degrees of freedom: this leads to an alternative formulation of the theory, now without a CS term. This undualized form will be useful for many purposes.

Let us first consider the simplest case of a single complex vison, as in model III. By the usual boson-vortex duality,⁶⁰ the dual of v is the monopole operator \mathcal{M}_b introduced below Eq. (4.6). This monopole operator carries charge $k=2$ under a_μ , and consequently we can write the theory for the two-component spinor z_α and the complex ‘‘Higgs’’ scalar \mathcal{M}_b . Thus a theory equivalent to Eq. (1.1) for models AIII and BIII is

$$\begin{aligned} \mathcal{L}_M = & \sum_{\alpha=1}^2 \{ |(\partial_\mu - ia_\mu)z_\alpha|^2 + s_z |z_\alpha|^2 \} + |(\partial_\mu + 2ia_\mu)\mathcal{M}_b|^2 \\ & - s_v |\mathcal{M}_b|^2 + u_z \left(\sum_{\alpha=1}^2 |z_\alpha|^2 \right)^2 + u_M |\mathcal{M}_b|^4 \\ & + v_M |\mathcal{M}_b|^2 \left(\sum_{\alpha=1}^2 |z_\alpha|^2 \right) + \lambda (\mathcal{M}_b \epsilon_{\alpha\beta\gamma\alpha} \partial_x z_\beta + \text{H.c.}). \end{aligned} \quad (5.1)$$

The λ term descends from Eq. (4.6) and is present only for model BIII. A closely related model, for a similar model, was obtained directly from the Schwinger boson formulation in Ref. 8. Note that we have (schematically) changed the sign of the ‘‘mass’’ term for \mathcal{M}_b from that for the vison v . This reflects the dual relation between the fields and the fact the v is condensed when \mathcal{M}_b is gapped, and vice versa. We note that the mapping between the CS theory in Eq. (1.1) and the non-CS theory in Eq. (5.1) is similar to that described for supersymmetric gauge theories in Ref. 50.

A similar (un)duality mapping can be applied to visons in models I and II. This mapping only works for the $g < 0$ (‘‘easy-plane’’) case of the theory in Eq. (4.1). In this case, the vison fields $v_{1,2}$ and the gauge field b_μ form an easy-plane CP¹ model, and so we can directly use the duality mappings of Ref. 61. The dual theory is yet another CP¹ model, with fields m_1 and m_2 and a gauge field c_μ . Here $m_{1,2}$ are merons in the vison CP¹ model, and the monopole in the b_μ field is^{3,61} $\mathcal{M}_b \sim m_1 m_2$. Thus a form of theory (4.1) for models AI, AII, BI, and BII with $g < 0$ is

$$\begin{aligned} \mathcal{L}_m = & \sum_{\alpha=1}^2 \{ |(\partial_\mu - ia_\mu)z_\alpha|^2 + s_z |z_\alpha|^2 \} + |(\partial_\mu + ia_\mu + ic_\mu)m_1|^2 \\ & + |(\partial_\mu + ia_\mu - ic_\mu)m_2|^2 - s_v \{ |m_1|^2 + |m_2|^2 \} \\ & + u_z \left(\sum_{\alpha=1}^2 |z_\alpha|^2 \right)^2 + u_m \{ |m_1|^2 + |m_2|^2 \}^2 + g_m |m_1|^2 |m_2|^2 \\ & + v_m \{ |m_1|^2 + |m_2|^2 \} \left(\sum_{\alpha=1}^2 |z_\alpha|^2 \right) \\ & + \lambda (m_1 m_2 \epsilon_{\alpha\beta\gamma\alpha} \partial_x z_\beta + \text{H.c.}). \end{aligned} \quad (5.2)$$

Again the λ term is present only for models BI and BII. Also the phase diagrams can be mapped by keeping in mind the dual relation between the visons $v_{1,2}$ and the merons $m_{1,2}$: the visons are condensed when the merons are gapped, and vice versa. Now we will turn to a description of the transitions for the various models, using the theories in Eqs. (1.1), (4.1), (5.1), and (5.2).

A. Phase transitions in model AI

1. Transition between Z_2 spin liquid and spiral spin state

This transition is known^{54–56} to be a three-dimensional (3D) O(4) transition, and the mutual CS theory does reproduce this O(4) universality class: in the Z_2 spin liquid, the vison is gapped. Therefore the gauge field a_μ is Higgsed by gauge field b_μ , and the U(1) gauge symmetry of a_μ is broken down to the Z_2 gauge symmetry. The critical point described by spinon z_α enjoys an enlarged O(4) symmetry.

2. Transition between Z_2 spin liquid and the VBS state

The nature of this transition depends on the sign of g . When $g < 0$, the Lagrangian describing this transition is

$$\mathcal{L} = \sum_{a=1}^2 |\partial_\mu v_a|^2 + r|v_a|^2 + u_v|v_a|^4 + (2u_v + g)|v_1|^2|v_2|^2 + g_8 v_1^4 v_2^4. \quad (5.3)$$

This Lagrangian describes two coupled 3D XY transitions. The coupling g_8 is clearly irrelevant at this 3D XY transition. The scaling dimension of $u_{12}=2u_v+g$ is $2/\nu-D<0$, and therefore is also irrelevant (ν is the critical exponent defined as $\xi \sim r^{-\nu}$ at the 3D XY transition, which is greater than $2/3$). So the transition between the Z_2 spin liquid and the VBS order is two copies of 3D XY transitions when $g<0$.

When $g>0$, the transition breaks the $U(1) \times Z_2$ symmetry. There can be one single first-order transition or two separate transitions, with 3D XY and 3D Ising universality class, respectively. If the triangular lattice is undistorted, $g=0$, there is one single transition between the Z_2 spin liquid and the VBS order, which belongs to 3D $O(4)$ universality class.

3. Transition between spiral spin state and the nematic +VBS state

If $g<0$ ($g>0$), this transition is described by a CP^1 Lagrangian with easy-plane (easy-axis) limit:

$$\mathcal{L} = \sum_{a=1}^2 |(\partial_\mu - ib_\mu)v_a|^2 + s_v|v_a|^2 + \dots \quad (5.4)$$

The eighth-order anisotropy term \mathcal{L}_8 is suppressed at this transition because the condensate of spinon is the Mott insulator phase of the flux of a_μ , which guarantees the conservation of total vison number.

4. Transition between VBS order and nematic order

This is a CP^1 transition described by spinon z_α and $U(1)$ gauge field a_μ . The eighth-order anisotropy term of vison $v_1^4 v_2^4 + \text{H.c.}$ violates the conservation of the flux of a_μ ; i.e., it corresponds to the instantons in the $2+1d$ space-time which creates/annihilates gauge fluxes. Because $k=2$ in Eq. (4.1), one flux of a_μ carries two visons; therefore \mathcal{L}_8 corresponds to a quadrupole process. If $g>0$, only one component of v_1 and v_2 condenses; the quadrupole process which involves both v_1 and v_2 is suppressed. However, if $g<0$, the quadrupole process is present, but expected to be irrelevant at the CP^1 critical point.³ We note here recent numerical studies of the CP^1 field theories, which include indications that this transition is weakly first order.^{61–66}

One other issue to notice is that the spinon velocity and the vison velocity do not have to be equal. Therefore in the CP^1 models described above, the velocity of matter fields and the velocity of gauge fields are essentially different. In the large- N limit, the $U(1)$ gauge field has scaling dimension of 1, and the one-loop self-energy of gauge field leads to the same velocity as the matter fields. The term with velocity anisotropy has scaling dimension of 4, and hence is irrelevant for large enough N .

B. Phase transitions in model AII

The phase transitions in model AII are similar to those in model AI. The only difference is that the eighth-order vison

term $\mathcal{L}_8 = g_8(v_1 v_2^*)^4 + \text{H.c.}$ conserves the total flux number of a_μ . Therefore there is no quadrupole process at the transition between the nematic order and the VBS order.

C. Phase transitions in model AIII

In model AIII, the transition between the spiral spin order and the Z_2 spin liquid is still $O(4)$, while the transition between the Z_2 spin liquid and the VBS order is a 3D XY transition (with an irrelevant eighth-order anisotropy), because there is only one flavor of vison.

The transition between the spiral spin order and the nematic spin order is an inverted 3D XY transition,⁶⁰ or a CP^0 model with one component of complex boson v coupled with the $U(1)$ gauge field b_μ . The transition between the nematic order and the VBS order is a CP^1 transition with irrelevant quadrupoles.

D. Phase transitions in models BI, BII, and BIII

The transitions in the models with spinon B are similar to the models with spinon A. The major concern is the effect of \mathcal{L}_x in Eq. (4.6) at the critical points. As discussed in Sec. IV D, this term is only effective when the vison is gapped or critical, such as, for instance, the transition between the Z_2 spin liquid and the spiral antiferromagnet. The theory for this transition with spinon A was the $O(4)$ model. With the term \mathcal{L}_x present in model B, we can redefine the spinon field using a x -dependent $O(4)$ rotation to absorb the linear x derivative.⁸ The transition is therefore seen to remain in the $O(4)$ class in model B.

At the transition between the Néel order and spiral order, the field theory is given by a $CP^{(N-1)}$ model with N flavors of visons ($N=1$ or 2) and gauge field b_μ . \mathcal{L}_x violates the conservation of spinon, and hence corresponds to a monopole term \mathcal{M}_b of b_μ . For simplicity, let us consider model BIII with one vison component as an example. Here we can analyze the Néel-spiral transition from the theory in Eq. (5.1) by condensing the monopole operator \mathcal{M}_b . We parametrize the spinon z as $z = e^{i\alpha}(e^{i\phi/2} \cos(\theta/2), e^{-i\phi/2} \sin(\theta/2))^t$, where α is a gauge-dependent phase angle coupled with the gauge field a_μ . Then the effective Lagrangian can be written as

$$L = (\partial_\mu \theta)^2 + (\sin \theta)^2 (\partial_\mu \phi)^2 + \tilde{\lambda} (\nabla_x \theta \text{Re}[\tilde{\mathcal{M}}_b] + \nabla_x \phi \sin \theta \text{Im}[\tilde{\mathcal{M}}_b]), \quad (5.5)$$

where $\tilde{\mathcal{M}}_b$ is the gauge-invariant monopole $\tilde{\mathcal{M}}_b = \mathcal{M}_b e^{2i\alpha}$. Integrating out the gapless spin waves ϕ and θ , a singular long-range dipole interaction is generated for field $\tilde{\mathcal{M}}_b$ with momentum dependence $q_x^2/(q^2 + \omega^2)$, which will change the relative scaling dimension between x and y, τ . The effective theory for XY field $\Psi \sim \tilde{\mathcal{M}}_b$ can be viewed as an effective $z=2$ theory with scaling dimension $\Delta[q_x] = 2\Delta[q_y] = 2\Delta[\omega] = 2$:

$$L_\Phi = \frac{q_x^2}{q_y^2 + \omega^2} |\Psi|^2 + (q_y^2 + \omega^2) |\Psi|^2 + g |\Psi|^4 + \dots \quad (5.6)$$

The upper critical dimension of this $z=2$ field theory is $d=2$. Therefore this transition will be a mean-field transition instead of a 3D XY transition.

For $N_v=2$ theories in Eq. (5.2), a similar dipolar term is generated at the quartic term for m_i . A more detailed analysis is required to determine the fate of this quartic term.

E. Isotropic triangular lattice

This subsection will briefly comment on the modifications of our results for the case of the isotropic triangular lattice, with $J'=J$ and full sixfold rotation symmetry. There is one more symmetry that needs to be considered: the $2\pi/3$ rotation. Under this rotation, the visons of model II transform as

$$R_{2\pi/3}: v_1 \rightarrow \frac{1}{\sqrt{2}} e^{-i\pi/4} v_1 + \frac{1}{\sqrt{2}} v_2, \quad v_2 \rightarrow -\frac{1}{\sqrt{2}} v_1 + \frac{1}{\sqrt{2}} e^{i\pi/4} v_2. \quad (5.7)$$

This PSG transformation is consistent with the enlarged U(1) gauge symmetry, while in model I, visons will be mixed with its complex conjugates. Therefore on the isotropic triangular lattice only model II of visons is consistent. Further, the spinon minima are located at the commensurate wave vectors $\vec{Q}=(2\pi/3, 0)$ and $-\vec{Q}=-(2\pi/3, 0)$. Therefore under translation spinons in model A will merely gain a phase factor, while in model B spinons will be mixed with their complex conjugates. Therefore on the isotropic triangular lattice, only model AII is consistent with the enlarged U(1) gauge symmetries.

In the mutual CS theory of model AII on the isotropic lattice, $g=0$, in the phase with both spinon and vison condensed, the VSB order parameter is described by the SU(2) vector $v^\dagger \sigma^a v$, which corresponds to degenerate stripe orders $V_{\vec{x}}$ and $V_{\vec{y}}$ in Eq. (4.4) and $V_z=v^\dagger \sigma^z v$ depicted in Fig. 7. These stripe orders are connected to each other through rotation $R_{2\pi/3}$. Notice that on the distorted triangular lattice, stripe order $V_{\vec{x}}$ has the same symmetry as the square lattice VBS order.

Because $g=0$, the global symmetry of vison up to the fourth-order term is SU(2) in the mutual CS theory, and O(4) in the theory with only visons. The GSM of the phase with both spinon and vison condensed is $S^2 \times S^2$ as far as the fourth-order terms are considered. Therefore the transition between the Z_2 spin liquid and the VBS order is a 3D O(4) transition,¹⁶ and the transition between the nematic/VBS order to the spiral order in phase diagram Fig. 8 is a CP¹ transition. The PSG of visons allow a sixth-order anisotropy term on the isotropic triangular lattice:¹⁶

$$L_6 = g_6 (v_1 v_2^5 + v_2 v_1^5 + \text{H.c.}). \quad (5.8)$$

This term corresponds to the triple monopole process in the dual picture, which annihilates/creates three fluxes of gauge field a_μ . This triple monopole is expected to be relevant when gauge field a_μ is gapless, which will likely drive the transition between the nematic/VBS and the VBS phase to a first-order transition.

F. Multicritical point, $s_z=s_v=0$

We now study the multicritical point with both spinons and visons gapless: this is the point M in Fig. 3. The most convenient way of studying M is likely via the non-CS theories in Eqs. (5.1) and (5.2), although these do not apply for the $g>0$ cases. This formulation should be amenable to direct numerical study.

For analytic results, the only available tool is the $1/N$ expansion; for this we may as well work with the original CS theory in Eq. (1.1). This expansion relies on the assumption that in Eq. (4.1) $N \sim N_v \sim k$ is large. The λ term in Eqs. (5.1) and (5.2) generalizes to terms with k powers of z_α , and these are surely irrelevant for large k . So we ignore the influence of \mathcal{L}_x for models B in the $1/N$ expansion.

A systematic $1/N$ expansion for the CP^(N-1) model has been calculated previously.^{67,68} The $1/N$ correction comes from the one-loop propagator of both the Lagrange multiplier λ and gauge field a_μ :

$$\mathcal{L} = \frac{1}{g} |(\partial_\mu - i a_\mu) z|^2 + i\lambda (|z|^2 - 1) + \dots \quad (5.9)$$

The one-loop propagators of λ and a_μ are

$$D_{\mu\nu} = \frac{1}{\Pi_A} \left(\delta_{\mu\nu} - \zeta \frac{q_\mu q_\nu}{q^2} \right), \quad \Pi_A = \frac{Np}{16},$$

$$D_\lambda = \frac{1}{\Pi_\lambda}, \quad \Pi_\lambda = \frac{Np}{8}. \quad (5.10)$$

For instance, we can calculate the anomalous dimension η_N of gauge-invariant operator $z^\dagger T^a z$ defined as $\Delta[z^\dagger T^a z] = (D - 2 + \eta_N)/2$, and T^a is one of the generators of SU(N) algebra. Note that this operator is the magnetic order parameter for model B, and the spin nematic order parameter for model A. In the CP^(N-1) model, the anomalous dimension η_N was calculated in detail in Ref. 68, and the result is

$$\eta_N = 1 + \frac{32}{3\pi^2 N} - \frac{128}{3\pi^2 N^2}. \quad (5.11)$$

The second term on the right-hand side of the equation above comes from the Lagrange multiplier, while the third term comes from the gauge field.

After including the vison multiplet v_a and mutual CS term, the λ propagator is unaffected, while the gauge field propagator is modified:

$$D_{\mu\nu} = \frac{1}{\tilde{\Pi}_A} \left(\delta_{\mu\nu} - \zeta \frac{q_\mu q_\nu}{q^2} \right), \quad \tilde{\Pi}_A = \frac{Np}{16} \left(1 + \frac{64k^2}{\pi^2 N^2} \right). \quad (5.12)$$

All the calculations can be carried out straightforwardly by replacing Π_A in Ref. 68 by $\tilde{\Pi}_A$. When $k \sim N$, the correction from the vison and mutual CS theory to the anomalous dimension η_N is on the order of $1/N$:

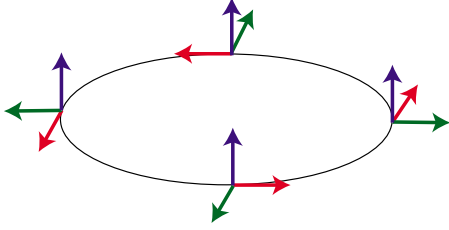


FIG. 10. (Color online) Schematic of the orientation of the orthogonal vectors \vec{n}_1 , \vec{n}_2 , and \vec{n}_3 around a vortex in the SO(3) GSM of the spiral antiferromagnet. One of the vectors has a constant orientation, while the other two precess by an angle of 2π .

$$\eta_N = 1 + \frac{32}{3\pi^2 N} - \frac{128}{3\pi^2 N} \times \frac{1}{1 + 64k^2/(\pi^2 N^2)}. \quad (5.13)$$

All the other critical exponents can be calculated in a similar way.

VI. BEYOND U(1) CHERN-SIMONS THEORIES

In Secs. IV and V, the global phase diagrams and nature of phase transitions were studied with the mutual CS theory. In this section we will try to look at these phases and transitions in a more intuitive and pictorial way. Let us start with the case with undistorted triangular lattice, which has a ground state with spiral antiferromagnetic order. This spiral order is described in terms of the z by Eq. (3.3).

Intuitively, to destroy magnetic order, the most straightforward way is to proliferate the topological defects in this magnetic order. The fundamental group of the GSM of spiral order is $\pi_1[\text{SO}(3)] = \mathbb{Z}_2$, which supports a topologically stable half vortex if rewritten in terms of z . These half vortices become full vortices of vectors \vec{n}_i , with $i=1, 2, 3$, in Eq. (3.3). These vortices can be most easily understood as an ordinary vortices of two of the three vectors \vec{n}_i , while keeping the third vector uniform in the whole $2d$ plane: see Fig. 10. The GSM of this state has isometry group SO(4). If the system has the enlarged O(4) symmetry at the microscopic level, all the vortices with different uniform vectors (UVs) will have the same energy. However, the underlying symmetry is only $\text{SU}(2) \times \text{PSG}$, so the energy of the vortices depends on the UV. The lattice symmetry guarantees that the vortices with different UVs have the same energy as long as the UVs can be transformed to each other through lattice symmetry transformations. There are in total three groups of vortices:

$$\begin{aligned} (1) \text{ UV: } \vec{n}_3, \\ (2) \text{ UV: } \vec{n}_1, \quad -\frac{1}{2}\vec{n}_1 \pm \frac{\sqrt{3}}{2}\vec{n}_2, \\ (3) \text{ UV: } \vec{n}_2, \quad \pm \frac{\sqrt{3}}{2}\vec{n}_1 - \frac{1}{2}\vec{n}_2. \end{aligned} \quad (6.1)$$

All the flavors of vortices in each group have the same energy, while there is no symmetry to protect the degeneracy

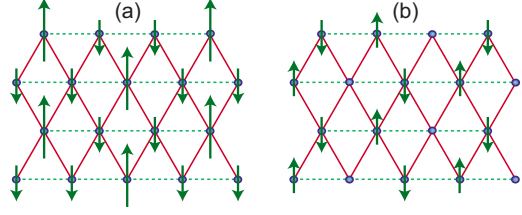


FIG. 11. (Color online) The remnant spin order pattern after proliferation of one single flavor of group 2 and 3 vortices in Eq. (6.1). (a) Proliferation of the first flavor in group 2; the spin pattern is up-down-down, and the GSM is $S^2 \times Z_3$. Notice that the moment of the up-spin site is twice as much as the down-spin site, so the total magnetization is zero. (b) Proliferation of first flavor in group 3; the spin pattern is up-down-zero with GSM $S^2 \times Z_3$.

between different groups. For instance, UV \vec{n}_3 can never be transformed into \vec{n}_1 because of their opposite behaviors under time-reversal transformation. The first group of vortex has only one flavor, and if we only proliferate this vortex flavor, the spin orders of \vec{n}_1 and \vec{n}_2 are destroyed, while the nematic order \vec{n}_3 is preserved. This leads to a state with GSM S^2 , and it is the situation described by the mutual CS theories AI, AII, and AIII. The second and third groups have more than one flavor of vortices, with different flavors of vortices connected to each other through lattice symmetry transformations. If all the flavors of vortices in group 2 or 3 condense, the magnetic order is completely destroyed, and we expect these vortices to drive a direct transition from the $\sqrt{3} \times \sqrt{3}$ antiferromagnetic spiral order to VBS order. The nature of this transition requires further study, and it cannot be naturally described by our mutual CS theory. In our theory, there are always two tuning parameters (s_z and s_v), and it would require some fine-tuning to induce a direct transition. A theory based on a mutual \mathbb{Z}_2 CS formalism has been proposed by another group⁶⁹ to describe this direct transition.

One can also condense one flavor of the second or the third group of vortices, which can be realized in the situation with strong repulsions between different flavors of vortices in one group. If the vortex with UV \vec{n}_1 is condensed, the vectors \vec{n}_2 and \vec{n}_3 are disordered, and the remnant magnetic order is the up-down-down state in Fig. 11(a) with zero total magnetization, and the GSM of this up-down-down state is $S^2 \times Z_3$. The S^2 corresponds to the direction of \vec{n}_1 , and the Z_3 corresponds to the choice of condensing the three flavors of vortices in the second group of Eq. (6.1), which are connected to each other via translation along the x axis. If vortex with UV \vec{n}_2 is condensed, the spin pattern becomes the up-down-zero state in Fig. 11(b), also with GSM $S^2 \times Z_3$. The transition driven by the condensation of vortices with UV \vec{n}_1 and \vec{n}_2 can no longer be described by the U(1) mutual CS theory because in the phase with both spinons and visons condensed, the physical order parameter of the remnant spin order should be U(1) gauge invariant. Thus now one needs a spinon z_α such that the UV $n_1 = z^\dagger \sigma^a z$. However, under translation, so-defined spinon z_α becomes a linear combination between z_α and $\epsilon_{\alpha\beta\gamma} z_\beta^*$, which violates the U(1) gauge symmetry.

To consistently describe the transition driven by proliferation of vortices with UV \vec{n}_1 and \vec{n}_2 , a theory based on mutual

Z_2 CS theory may be applicable, similar to the Z_2 CS formalism proposed for cuprates³⁶ where the spinons and half vortices of the superconducting phase are coupled together through mutual Z_2 CS fields. On the distorted triangular lattice antiferromagnets examined in this work, the mutual Z_2 gauge field also imposes the correct semionic statistics between the spinon and vison. However the Z_2 gauge field can only be conveniently formulated on the lattice. Therefore we are unable to comment on all the universal properties of the transitions described by the mutual Z_2 CS theory.

If the triangular lattice is distorted, the spin spiral state becomes incommensurate, and the vector \vec{n}_1 and \vec{n}_2 can be transformed to each other via lattice translation. Therefore there are only two groups of vortices:

$$(1) \text{ UV}:\vec{n}_3,$$

$$(2) \text{ UV}:\vec{n}_1, \text{ rotation of } \vec{n}_1 \text{ around } \vec{n}_3. \quad (6.2)$$

The second group of vortices has an infinite number of flavors, and if one of these flavors proliferates, then the spin state becomes a collinear incommensurate spin-density wave, which has GSM $S^2 \times S^1$. The S^2 corresponds to the remnant spin collinear order, while the S^1 corresponds to translation along \hat{x} of the incommensurate wave vector.

VII. CONCLUSIONS AND EXPERIMENTAL IMPLICATIONS

This paper has described examples of a general approach to describing the phases and quantum phase transitions of $S=1/2$ antiferromagnets in two dimensions. Our examples were limited to models on the lattice in Fig. 1 because of its experimental importance. However, we expect that similar analysis should be useful, e.g., on the kagome lattice. Our main results are summarized in phase diagrams, such as that in Fig. 2. The same phase diagram was obtained earlier⁸ in a more direct microscopic mean-field theory, but the nature of the phase transitions and possible multicritical point was left open. Our present dual approach also immediately yields the required critical-field theories.

One of the transitions in our phase diagram in Fig. 2 is the Néel-VBS transition, which is described by a CP^1 field theory. This transition has been the focus of much recent numerical work.^{61–66} The numeric results on the $S=1/2$ quantum antiferromagnet strongly support its effective description in terms of the CP^1 field theory. However, some results^{64,65} on system sizes larger than 50×50 indicate that the transition in the CP^1 model may well be weakly first order. The multicritical point M has additional flavors of matter fields, and these make it less likely that M is first order. Consequently it would be useful to study M numerically using the theories in Eqs. (5.1) and (5.2): this will help in describing M and the phase diagram in its immediate vicinity. This study can be done with or without the λ coupling in Eqs. (5.1) and (5.2).

As mentioned in Sec. I, a series of measurements on the distorted triangular lattice materials $X[\text{Pd}(\text{dmit})_2]_2$ with different anisotropic couplings J'/J reveal a possible direct

transition between the Néel order and the VBS state. One particular material with $X=\text{EtMe}_3\text{Sb}$ was suggested to be close to the quantum critical point. In our mutual CS theory, as well as the previously proposed deconfined critical point,³ this transition is described by the CP^1 model with irrelevant quadrupole operators. The quantum critical behaviors at finite temperature can be measured in material $\text{EtMe}_3\text{Sb}[\text{Pd}(\text{dmit})_2]_2$. For instance, the nuclear-magnetic-resonance (NMR) relaxation rate $1/T_1$ scales as $1/T_1 \sim T^{\eta_N}$, where η_N is the anomalous dimension of the Néel order parameter at the CP^1 fixed point. Even if the transition in the CP^1 model is ultimately weakly first order, the critical regime could be observable at intermediate T , and compared to numerical estimates^{62,63,66} of η_N .

We conclude by commenting on the recent interpretation in Ref. 32 of experimental observations on the spin-liquid compound $\kappa\text{-(ET)}_2\text{Cu}_2(\text{CN})_3$. It was suggested in Ref. 32 that the very-low- T nuclear magnetic resonance was controlled by the $O(4)$ criticality between the spiral and Z_2 spin-liquid states, while the intermediate-temperature NMR could be modeled by a multicritical point where both the spinons and visons are gapless. Crucial to this interpretation was the requirement that the anomalous dimension of the magnetic order parameter, η_N , was smaller at the latter multicritical point than at the low- T $O(4)$ critical point.

Here, we have provided examples of such multicritical points, such as point M in Fig. 2. For spinons in model B, the magnetic order parameter is $z^\dagger T^a z$, and its anomalous dimension was computed in Sec. V F, where we found the result in Eq. (5.13). An important feature of this result is that the $U(1)$ gauge fluctuations reduce the value of η_N from that obtained in the theory without the $U(1)$ gauge field. The latter describes the $O(4)$ transition between the spiral antiferromagnet and the Z_2 spin liquid. Thus model B spinons do fulfill the requirements for the experimental interpretation stated in Ref. 32.

On the other hand, in spinon model A, the order parameter $z^\dagger T^a z$ represents the nematic order parameter, while the other gauge-invariant spinon-monopole composite $z^\dagger \sigma^y \sigma^a z \mathcal{M}_b$ represents the spiral order parameter. In the case with large N_b , the scaling dimension of \mathcal{M}_b is expected to scale linearly with N_b . Hence to systematically calculate the scaling dimension of $z^\dagger \sigma^y \sigma^a z \mathcal{M}_b$, we need an analytical technique beyond the $1/N$ expansion.

In conclusion, we have proposed a unified theory in the mutual CS formalism to describe all the magnetic phases observed in a series of organic compounds, and discussed the phase transitions between these phases. Experimental implications for organic compounds in the $X[\text{Pd}(\text{dmit})_2]_2$ series and the $\kappa\text{-(ET)}_2\text{Z}$ series were also discussed.

ACKNOWLEDGMENTS

We thank L. Balents, M. P. A. Fisher, R. Kato, I. Klebanov, P. A. Lee, Y. Qi, T. Senthil, Y. Shimizu, M. Yamashita, and X. Yin for useful discussions. This research was supported by the NSF under Grant No. DMR-0757145, by the FQXi foundation.

- ¹N. Read and S. Sachdev, *Phys. Rev. Lett.* **62**, 1694 (1989).
- ²N. Read and S. Sachdev, *Phys. Rev. B* **42**, 4568 (1990).
- ³T. Senthil, A. Vishwanath, L. Balents, S. Sachdev, and M. P. A. Fisher, *Science* **303**, 1490 (2004); T. Senthil, L. Balents, S. Sachdev, A. Vishwanath, and M. P. A. Fisher, *Phys. Rev. B* **70**, 144407 (2004).
- ⁴O. A. Starykh and L. Balents, *Phys. Rev. Lett.* **98**, 077205 (2007).
- ⁵M. Kohno, O. A. Starykh, and L. Balents, *Nat. Phys.* **3**, 790 (2007).
- ⁶N. Read and S. Sachdev, *Phys. Rev. Lett.* **66**, 1773 (1991).
- ⁷R. A. Jalabert and S. Sachdev, *Phys. Rev. B* **44**, 686 (1991); S. Sachdev and K. Damle, *J. Phys. Soc. Jpn.* **69**, 2712 (2000).
- ⁸S. Sachdev and N. Read, *Int. J. Mod. Phys. B* **5**, 219 (1991).
- ⁹S. Sachdev, *Phys. Rev. B* **45**, 12377 (1992).
- ¹⁰Zheng Weihong, R. H. McKenzie, and R. P. Singh, *Phys. Rev. B* **59**, 14367 (1999).
- ¹¹G. Misguich, C. Lhuillier, B. Bernu, and C. Waldtmann, *Phys. Rev. B* **60**, 1064 (1999).
- ¹²W. LiMing, G. Misguich, P. Sindzingre, and C. Lhuillier, *Phys. Rev. B* **62**, 6372 (2000).
- ¹³O. I. Motrunich, *Phys. Rev. B* **72**, 045105 (2005).
- ¹⁴D. N. Sheng, O. I. Motrunich, S. Trebst, E. Gull, and M. P. A. Fisher, *Phys. Rev. B* **78**, 054520 (2008).
- ¹⁵D. S. Rokhsar and S. A. Kivelson, *Phys. Rev. Lett.* **61**, 2376 (1988).
- ¹⁶R. Moessner and S. L. Sondhi, *Phys. Rev. B* **63**, 224401 (2001).
- ¹⁷T. Nakamura, T. Takahashi, S. Aonuma, and R. Kato, *J. Mater. Chem.* **11**, 2159 (2001).
- ¹⁸M. Tamura and R. Kato, *J. Phys.: Condens. Matter* **14**, L729 (2002).
- ¹⁹S. Ohira, M. Tamura, R. Kato, I. Watanabe, and M. Iwasaki, *Phys. Rev. B* **70**, 220404(R) (2004).
- ²⁰M. Tamura, A. Nakao, and R. Kato, *J. Phys. Soc. Jpn.* **75**, 093701 (2006).
- ²¹Y. Shimizu, H. Akimoto, H. Tsujii, A. Tajima, and R. Kato, *Phys. Rev. Lett.* **99**, 256403 (2007).
- ²²Y. Shimizu, H. Akimoto, H. Tsujii, A. Tajima, and R. Kato, *J. Phys.: Condens. Matter* **19**, 145240 (2007).
- ²³T. Itou, A. Oyamada, S. Maegawa, M. Tamura, and R. Kato, *Phys. Rev. B* **77**, 104413 (2008).
- ²⁴B. J. Powell and R. H. McKenzie, *J. Phys.: Condens. Matter* **18**, R827 (2006).
- ²⁵K. Miyagawa, A. Kawamoto, Y. Nakazawa, and K. Kanoda, *Phys. Rev. Lett.* **75**, 1174 (1995).
- ²⁶Y. Shimizu, K. Miyagawa, K. Kanoda, M. Maesato, and G. Saito, *Phys. Rev. Lett.* **91**, 107001 (2003).
- ²⁷Y. Shimizu, K. Miyagawa, K. Kanoda, M. Maesato, and G. Saito, *Phys. Rev. B* **73**, 140407(R) (2006).
- ²⁸S. Yamashita, Y. Nakazawa, M. Oguni, Y. Oshima, H. Nojiri, Y. Shimizu, K. Miyagawa, and K. Kanoda, *Nat. Phys.* **4**, 459 (2008).
- ²⁹M. Yamashita, H. Nakata, Y. Kasahara, S. Fujimoto, T. Shibauchi, Y. Matsuda, T. Sasaki, N. Yoneyama, and N. Kobayashi, 25th International Conference on Low Temperature Physics, Amsterdam, 9 August 2008 (unpublished).
- ³⁰S.-S. Lee, P. A. Lee, and T. Senthil, *Phys. Rev. Lett.* **98**, 067006 (2007).
- ³¹Y. Qi and S. Sachdev, *Phys. Rev. B* **77**, 165112 (2008).
- ³²Y. Qi, C. Xu, and S. Sachdev, arXiv:0809.0694 (unpublished).
- ³³J. O. Fjærestad, W. Zheng, R. R. P. Singh, R. H. McKenzie, and R. Coldea, *Phys. Rev. B* **75**, 174447 (2007).
- ³⁴R. Coldea, D. A. Tennant, A. M. Tsvelik, and Z. Tylczynski, *Phys. Rev. Lett.* **86**, 1335 (2001).
- ³⁵X. G. Wen, *Phys. Rev. B* **44**, 2664 (1991).
- ³⁶T. Senthil and M. P. A. Fisher, *Phys. Rev. B* **62**, 7850 (2000).
- ³⁷A. Y. Kitaev, *Ann. Phys. (N.Y.)* **303**, 2 (2003).
- ³⁸X. G. Wen, *Phys. Rev. Lett.* **90**, 016803 (2003).
- ³⁹M. Freedman, C. Nayak, K. Shtengel, K. Walker, and Z. Wang, *Ann. Phys. (N.Y.)* **310**, 428 (2004).
- ⁴⁰F. Wang and A. Vishwanath, *Phys. Rev. B* **74**, 174423 (2006).
- ⁴¹G. Misguich and F. Mila, *Phys. Rev. B* **77**, 134421 (2008).
- ⁴²N. Read and B. Chakraborty, *Phys. Rev. B* **40**, 7133 (1989).
- ⁴³S.-P. Kou, M. Levin, and X.-G. Wen, *Phys. Rev. B* **78**, 155134 (2008).
- ⁴⁴S.-P. Kou, X.-L. Qi, and Z.-Y. Weng, *Phys. Rev. B* **71**, 235102 (2005).
- ⁴⁵J. Bagger and N. Lambert, *Phys. Rev. D* **75**, 045020 (2007); **77**, 065008 (2008).
- ⁴⁶A. Gustavsson, arXiv:0709.1260 (unpublished).
- ⁴⁷M. Van Raamsdonk, *J. High Energy Phys.* **05** (2008) 105.
- ⁴⁸O. Aharony, O. Bergman, D. L. Jafferis, and J. Maldacena, *J. High Energy Phys.* **10**, (2008) 091.
- ⁴⁹M. Benna, I. Klebanov, T. Klose, and M. Smedback, *J. High Energy Phys.* **09** (2008) 072.
- ⁵⁰D. L. Jafferis and X. Yin, arXiv:0810.1243 (unpublished).
- ⁵¹S. Sachdev and X. Yin, arXiv:0808.0191 (unpublished).
- ⁵²L. Balents and M. P. A. Fisher, *Phys. Rev. B* **71**, 085119 (2005).
- ⁵³P. W. Anderson, *Phys. Rev.* **86**, 694 (1952).
- ⁵⁴P. Azaria, B. Delamotte, and T. Jolicoeur, *Phys. Rev. Lett.* **64**, 3175 (1990).
- ⁵⁵A. V. Chubukov, T. Senthil, and S. Sachdev, *Phys. Rev. Lett.* **72**, 2089 (1994).
- ⁵⁶S. V. Isakov, T. Senthil, and Y. B. Kim, *Phys. Rev. B* **72**, 174417 (2005).
- ⁵⁷S. Sachdev, *Rev. Mod. Phys.* **75**, 913 (2003).
- ⁵⁸C. Lannert, M. P. A. Fisher, and T. Senthil, *Phys. Rev. B* **63**, 134510 (2001).
- ⁵⁹L. Balents, L. Bartosch, A. Burkov, S. Sachdev, and K. Sengupta, *Phys. Rev. B* **71**, 144508 (2005).
- ⁶⁰C. Dasgupta and B. I. Halperin, *Phys. Rev. Lett.* **47**, 1556 (1981).
- ⁶¹O. I. Motrunich and A. Vishwanath, *Phys. Rev. B* **70**, 075104 (2004).
- ⁶²A. W. Sandvik, *Phys. Rev. Lett.* **98**, 227202 (2007).
- ⁶³R. G. Melko and R. K. Kaul, *Phys. Rev. Lett.* **100**, 017203 (2008); R. K. Kaul and R. G. Melko, *Phys. Rev. B* **78**, 014417 (2008).
- ⁶⁴F.-J. Jiang, M. Nyfeler, S. Chandrasekharan, and U.-J. Wiese, arXiv:0710.3926 (unpublished).
- ⁶⁵A. B. Kuklov, M. Matsumoto, N. V. Prokof'ev, B. V. Svistunov, and M. Troyer, *Phys. Rev. Lett.* **101**, 050405 (2008).
- ⁶⁶O. I. Motrunich and A. Vishwanath, arXiv:0805.1494 (unpublished).
- ⁶⁷V. Yu. Irkhin, A. A. Katanin, and M. I. Katsnelson, *Phys. Rev. B* **54**, 11953 (1996).
- ⁶⁸R. K. Kaul and S. Sachdev, *Phys. Rev. B* **77**, 155105 (2008).
- ⁶⁹S. Bhattacharjee and T. Senthil (unpublished).